Quark deconfinement and implications for the radius and the limiting mass of compact stars

Ignazio Bombaci[1], Irene Parenti[1], and Isaac Vidaña[1]

ABSTRACT

We study the consequences of the hadron-quark deconfinement phase transition in stellar compact objects when finite size effects between the deconfined quark phase and the hadronic phase are taken into account. We show that above a threshold value of the central pressure (gravitational mass) a neutron star is metastable to the decay (conversion) to a hybrid neutron star or to a strange star. The *mean-life time* of the metastable configuration dramatically depends on the value of the stellar central pressure. We explore the consequences of the metastability of "massive" neutron stars and of the existence of stable compact quark stars (hybrid neutron stars or strange stars) on the concept of limiting mass of compact stars. We discuss the implications of our scenario on the interpretation of the stellar mass and radius extracted from the spectra of several X-ray compact sources. Finally, we show that our scenario implies, as a natural consequence a two step-process which is able to explain the inferred "delayed" connection between supernova explosions and GRBs, giving also the correct energy to power GRBs.

Subject headings: elementary particles – dense matter – stars: neutron – gamma rays: bursts

1. Introduction

One of the most fascinating enigma in modern astrophysics concerns the true nature of the ultra-dense compact objects called *neutron stars* (NS). The bulk properties and the internal structure of these stars chiefly depends upon the equation of state (EOS) of dense hadronic matter. Different models for the EOS of dense matter predict a neutron star maximum mass (M_{max}) in the range of 1.4 – 2.2 $M_{\odot}$, and a corresponding central density

[1]Dipartimento di Fisica "Enrico Fermi", Universitá di Pisa, and INFN Sezione Pisa, via Buonarroti 2, I-56127 Pisa, Italy.

in range of 4 – 8 times the saturation density ($\rho_0 \sim 2.8 \times 10^{14}$g/cm^3) of nuclear matter (e.g. Shapiro & Teukolsky 1983; Haensel 2003). In the case of a star with $M \sim 1.4\ M_\odot$, different EOS models predict a radius in the range of 7 – 16 km (Shapiro & Teukolsky 1983; Haensel 2003; Dey et al. 1998).

In a simplistic and conservative picture the core of a neutron star is modeled as a uniform fluid of neutron rich nuclear matter in equilibrium with respect to the weak interaction (β-stable nuclear matter). However, due to the large value of the stellar central density and to the rapid increase of the nucleon chemical potentials with density, hyperons (Λ, Σ^-, Σ^0, Σ^+, Ξ^- and Ξ^0 particles) are expected to appear in the inner core of the star. Other *exotic* phases of hadronic matter such as a Bose-Einstein condensate of negative pion (π^-) or negative kaon (K^-) could be present in the inner part of the star.

According to Quantum Chromodynamics (QCD) a phase transition from hadronic matter to a deconfined quark phase should occur at a density of a few times nuclear matter saturation density. Consequently, the core of the more massive neutron stars is one of the best candidates in the Universe where such deconfined phase of quark matter (QM) could be found. This possibility was realized by several researchers soon after the introduction of quarks as the fundamentals building blocks of hadrons (Ivanenko & Kurdgelaidze 1969; Itoh 1970; Iachello et al. 1974; Collins & Perry 1975; Baym & Chin 1976; Keister & Kisslinger 1976). Since β-stable hadronic matter posses two conserved "charges" (*i.e.,* electric charge and baryon number) the quark-deconfinement phase transition proceeds through a mixed phase over a finite range of pressures and densities according to the Gibbs' criterion for phase equilibrium (Glendenning 1992; Müller & Serot 1995). At the onset of the mixed phase, quark matter droplets form a Coulomb lattice embedded in a sea of hadrons and in a roughly uniform sea of electrons and muons. As the pressure increases various geometrical shapes (rods, plates) of the less abundant phase immersed in the dominant one are expected. Finally the system turns into uniform quark matter at the highest pressure of the mixed phase (Heiselberg et al. 1993; Voskresensky et al. 2003). Compact stars which possess a "quark matter core" either as a mixed phase of deconfined quarks and hadrons or as a pure quark matter phase are called *Hybrid Neutron Stars* or shortly *Hybrid Stars* (HyS) (Glendenning 1996; Drago & Lavagno 2001). In the following of this paper, the more *conventional* neutron stars in which no fraction of quark matter is present, will be referred to as *pure Hadronic Stars* (HS).

Even more intriguing than the existence of a quark core in a neutron star, is the possible existence of a new family of compact stars consisting completely of a deconfined mixture of *up* (u), *down* (d) and *strange* (s) quarks (together with an appropriate number of electrons to guarantee electrical neutrality) satisfying the Bodmer–Witten hypothesis (Bodmer 1971;

Witten 1984; see also Terazawa 1979). Such compact stars have been called *strange quark stars* or shortly *strange stars* (SS) (Alcock et al. 1986; Haensel et al. 1986) and their constituent matter as *strange quark matter* (SQM) (Farhi & Jaffe 1984; Madsen 1999). Presently there is no unambiguous proof about the existence of strange stars, however, a sizable amount of observational data collected by the new generations of X-ray satellites, is providing a growing body of evidence for their possible existence (Bombaci 1997; Cheng et al. 1998; Li et al. 1999a; Li et al. 1999b; Xu 2002; Drake et al. 2002). It is generally believed that the unambiguous identification of a strange star will imply that all pulsars must be strange stars. In the present work we argue that the possible existence of strange stars does not conflict with the existence of *conventional* neutron stars (pure Hadronic Stars).

Present accurate determinations of compact star masses in radio pulsar binaries (Thorsett & Chakrabarty 1999) permit to rule out only *extremely soft* EOS, *i.e.* those giving M_{max} less than about 1.45 $M_{\odot}$. However, in at least two accreting X-ray binaries it has been found evidence for compact stars with higher masses. The first of these star is Vela X-1, with a reported mass $1.88 \pm 0.13 M_{\odot}$ (Quaintrell et al. 2003), the second is Cygnus X-2, with a reported mass of $1.78 \pm 0.23 M_{\odot}$ (Orosz & Kuulkers 1999). Unfortunately, mass determinations in X-ray binaries are affected by large uncertainties (van Kerkwijk et al. 1995), therefore the previous quoted "high mass values" should always be handled with care. In addition to mass determination, existing observational data on the spin frequency of millisecond pulsars and on the thermal evolution of neutron stars do not put severe constraints on the EOS of dense matter. Fortunately, this situation is improving in the last few years. In fact, the extraordinary spectroscopic capabilities of the instruments on board Chandra X-ray and XMM-Newton satellites, are giving the unique possibility to perform accurate measurements of the gravitational red-shift in the spectral lines of a few compact X-ray sources. This provide informations on the mass to radius ratio for compact stars and will help us to understand the true nature of these compact objects.

In this work we study the effects of the hadron-quark deconfinement phase transition in stellar compact objects. We show that when finite size effects at the interface between the quark- and the hadron-phase are taken into account, pure Hadronic Stars, above a threshold value of the central pressure (gravitational mass), are metastable to the *decay* (*conversion*) to hybrid neutron stars or to strange stars (depending on the properties of EOS for quark matter). The *mean-life time* of the metastable stellar configuration is related to the quantum nucleation time to form a drop of quark matter in the stellar center, and dramatically depends on the value of the stellar central pressure. We explore the consequences of the metastability of "massive" pure Hadronic Stars and the existence of stable compact quark stars (hybrid neutron stars or strange stars) on the concept of limiting mass of compact stars. Next, we discuss the implications of our scenario in the interpretation of the mass-radius

constraints extracted from the spectra of several X-ray compact sources. Finally, we discuss the implications of our scenario for Gamma Ray Bursts.

2. Quantum nucleation of quark matter in hadronic stars

Nucleation of quark matter in neutron stars has been studied by many authors. Most of the earlier studies on this subject (Horvath et al. 1992; Horvath 1994; Olesen & Madsen 1994; Heiselberg 1995; Grassi 1998) have been restricted to the case of thermal nucleation in hot and dense hadronic matter. In these studies, it was found that the prompt formation of a critical size drop of quark matter via thermal activation is possible above a temperature of about 2 – 3 MeV. As a consequence, it was inferred that pure hadronic stars are converted to strange stars or to hybrid stars within the first seconds after their birth. It was also suggested that the large amount of energy liberated in this process could play a crucial role in type-II supernova explosions (Benvenuto & Horvath 1989).

All the studies on quark matter nucleation mentioned above, have neglected an important physical aspect which charecterizes dense matter in a newly born *neutron star*: the trapping of neutrinos in the stellar core. Neutrino trapping has a sizeable influence on the *stiffness* of the EOS and, consequently, on the structural properties of the protoneutron star (Bombaci 1996; Prakash et al. 1997). In particular, it has been found that neutrino trapping significantly shifts the critical baryon density for the quark deconfinement phase transition to higher values with respect to the neutrino-free case (Prakash et al. 1997; Lugones & Benvenuto 1998). In addition, neutrino trapping decreases the value of the central density of the stellar maximum mass configuration with respect to the neutrino-free case (Prakash et al. 1997). Thus, the formation of a metastable supercompressed phase of hadronic matter is strongly inhibited in a protoneutron star. A detailed study of quark matter nucleation in hot and dense hadronic matter with trapped neutrinos will be presented in a forthcoming work (Bombaci et al. 2004).

In the present paper, we assume that the compact star survives the early stages of its evolution as a pure hadronic star, and we study quark matter nucleation in cold (T = 0) neutrino-free hadronic matter.

In bulk matter the quark-hadron mixed phase begins at the *static transition point* defined according to the Gibbs' criterion for phase equilibrium

$$\mu_H = \mu_Q \equiv \mu_0 \,, \qquad P_H(\mu_0) = P_Q(\mu_0) \equiv P_0 \tag{1}$$

where

$$\mu_H = \frac{\varepsilon_H + P_H}{n_{b,H}}\,, \qquad\qquad \mu_Q = \frac{\varepsilon_Q + P_Q}{n_{b,Q}} \tag{2}$$

are the chemical potentials for the hadron and quark phase respectively, ε_H (ε_Q), P_H (P_Q) and $n_{b,H}$ ($n_{b,Q}$) denote respectively the total (*i.e.,* including leptonic contributions) energy density, the total pressure and baryon number density for the hadron (quark) phase, in the case of cold matter.

Let us now consider the more realistic situation in which one takes into account the energy cost due to finite size effects in creating a drop of deconfined quark matter in the hadronic environment. As a consequence of these effects, the formation of a critical-size drop of QM is not immediate and it is necessary to have an overpressure $\Delta P = P - P_0$ with respect to the static the transition point. Thus, above P_0, hadronic matter is in a metastable state, and the formation of a real drop of quark matter occurs via a quantum nucleation mechanism. A sub-critical (virtual) droplet of deconfined quark matter moves back and forth in the potential energy well separating the two matter phases (see discussion below) on a time scale $\nu_0^{-1} \sim 10^{-23}$ seconds, which is set by the strong interactions. This time scale is many orders of magnitude shorter than the typical time scale for the weak interactions, therefore quark flavor must be conserved during the deconfinement transition. We will refer to this form of deconfined matter, in which the flavor content is equal to that of the β-stable hadronic system at the same pressure, as the Q*-phase. Soon afterwards a critical size drop of quark matter is formed the weak interactions will have enough time to act, changing the quark flavor fraction of the deconfined droplet to lower its energy, and a droplet of β-stable SQM is formed (hereafter the Q-phase). For example, if quark deconfinement occurs in β-stable nuclear matter (non-strange hadronic matter), it will produce a two-flavor (u and d) quark matter droplet having

$$n_u/n_d = (1 + x_p)/(2 - x_p)\,, \tag{3}$$

n_u and n_d being the *up* and *down* quark number densities respectively, and x_p the proton fraction in the β-stable hadronic phase. In the more general case in which the hadronic phase has a strangeness content (*e.g.,* hyperonic matter), the deconfinement transition will form a droplet of strange matter with a flavor content equal to that of the β-stable hadronic

system at the same pressure, according to the relation:

$$\begin{pmatrix} x_u \\ x_d \\ x_s \end{pmatrix} = \begin{pmatrix} 2 & 1 & 1 & 2 & 1 & 0 & 1 & 0 \\ 1 & 2 & 1 & 0 & 1 & 2 & 0 & 1 \\ 0 & 0 & 1 & 1 & 1 & 1 & 2 & 2 \end{pmatrix} \begin{pmatrix} x_p \\ x_n \\ x_\Lambda \\ x_{\Sigma^+} \\ x_{\Sigma^0} \\ x_{\Sigma^-} \\ x_{\Xi^0} \\ x_{\Xi^-} \end{pmatrix} , \tag{4}$$

where $x_i = n_i/n_b$ are the concentrations of the different particle species.

In the present work, we have adopted rather common models for describing both the hadronic and the quark phase of dense matter. For the hadronic phase we used models which are based on a relativistic lagrangian of hadrons interacting via the exchange of sigma, rho and omega mesons. The parameters adopted are the standard ones (Glendenning & Moszkowski 1991). Hereafter we refer to this model as the GM equation of state (EOS). For the quark phase we have adopted a phenomenological EOS (Farhi & Jaffe 1984) which is based on the MIT bag model for hadrons. The parameters here are: the mass m_s of the strange quark, the so-called pressure of the vacuum B (bag constant) and the QCD structure constant α_s. For all the quark matter model used in the present work, we take $m_u = m_d = 0$, $m_s = 150$ MeV and $\alpha_s = 0$.

In the left panel of Fig. 1, we show the chemical potentials, defined according to Eq. (2), as a function of the total pressure for the three phases of matter (H, Q*, and Q) discussed above. In the right panel of the same figure, we plot the energy densities for the H- and Q-phase as a function of the corresponding baryon number densities. Both panels in Fig. 1 are relative to the GM3 model for the EOS for the H-phase and to the MIT bag model EOS for the Q and Q* phases with $B = 152.45$ MeV/fm^3.

To calculate the nucleation rate of quark matter in the hadronic medium we use the Lifshitz–Kagan quantum nucleation theory (Lifshitz & Kagan 1972) in the relativistic form given by Iida & Sato (1997). The QM droplet is supposed to be a sphere of radius $\mathcal{R}$ and its quantum fluctuations are described by the lagrangian

$$L(\mathcal{R}, \dot{\mathcal{R}}) = -\mathcal{M}(\mathcal{R})c^2\sqrt{1 - (\dot{\mathcal{R}}/c)^2} + \mathcal{M}(\mathcal{R})c^2 - U(\mathcal{R}) \,, \tag{5}$$

where $\mathcal{M}(\mathcal{R})$ is the effective mass of the QM droplet, and $U(\mathcal{R})$ its potential energy. Within the Lifshitz–Kagan quantum nucleation theory, one assumes that the phase boundary (*i.e.* the droplet surface) moves slowly compared to the high sound velocity of the medium ($\dot{\mathcal{R}} <<$

$v_s \sim c$). Thus the number density of each phase adjust adiabatically to the fluctuations of the droplet radius, and the system retains pressure equilibrium between the two phases. Thus, the droplet effective mass is given by (Lifshitz & Kagan 1972; Iida & Sato 1997)

$$\mathcal{M}(\mathcal{R}) = 4\pi\rho_H\Big(1 - \frac{n_{b,Q*}}{n_{b,H}}\Big)^2\mathcal{R}^3\,, \tag{6}$$

ρ_H being the hadronic mass density, $n_{b,H}$ and $n_{b,Q*}$ are the baryonic number densities at a same pressure in the hadronic and Q*-phase, respectively. The potential energy is given by (Lifshitz & Kagan 1972; Iida & Sato 1997)

$$U(\mathcal{R}) = \frac{4}{3}\pi\mathcal{R}^3 n_{b,Q*}(\mu_{Q*} - \mu_H) + 4\pi\sigma\mathcal{R}^2 + 8\pi\gamma\mathcal{R}\,, \tag{7}$$

where μ_H and μ_{Q*} are the hadronic and quark chemical potentials at a fixed pressure P and σ is the surface tension for the surface separating the quark phase from the hadronic phase. The value of the surface tension σ is poorly known, and typical values used in the literature range within 10–50 MeV/fm^2 (Heiselberg et al. 1993; Iida & Sato 1997). The third term in Eq. (7), $E_{curv} = 8\pi\gamma\mathcal{R}$, is the so called *curvature energy*. It has been shown that E_{curv} plays an important role in the thermal nucleation process of quark matter in hot hadronic matter (Horvath 1994; Olesen & Madsen 1994). Specifically, the curvature term increases the minimum temperature for thermal nucleation with respect to the case $\gamma = 0$ (Horvath 1994). Most of the results reported in the present study have been obtained taking $\gamma = 0$ in Eq. (7). In a few cases (see Tab. 3), we considered $\gamma \neq 0$ to investigate the influence of the curvature energy on quantum nucleation in cold hadronic matter.

In the previous expression (7) for the droplet potential energy, we neglected the terms connected with the electrostatic energy. Detailed calculations by Iida & Sato (1997) have demonstrated that the contribution of these terms to Eq. (7) can be safely omitted since the screening action by leptons nearly compensate the effect of the positive charged droplet.

The process of formation of a bubble having a critical radius, can be computed using a semiclassical approximation. The procedure is rather straightforward. First one computes, using the well known Wentzel–Kramers–Brillouin (WKB) approximation, the ground state energy E_0 and the oscillation frequency ν_0 of the virtual QM drop in the potential well $U(\mathcal{R})$. Then it is possible to calculate in a relativistic framework the probability of tunneling as (Iida & Sato 1997)

$$p_0 = \exp\Big[-\frac{A(E_0)}{\hbar}\Big] \tag{8}$$

where A is the action under the potential barrier

$$A(E) = \frac{2}{c}\int_{\mathcal{R}_-}^{\mathcal{R}_+}\big\{[2\mathcal{M}(\mathcal{R})c^2 + E - U(\mathcal{R})]\times[U(\mathcal{R}) - E]\big\}^{1/2}\,d\mathcal{R}\,, \tag{9}$$

$\mathcal{R}_\pm$ being the classical turning points.

The nucleation time is then equal to

$$\tau = (\nu_0 p_0 N_c)^{-1} \,, \tag{10}$$

where N_c is the number of virtual centers of droplet formation in the innermost region of the star. Following the simple estimate given in Iida & Sato (1997), we take $N_c = 10^{48}$. The uncertainty in the value of N_c is expected to be within one or two orders of magnitude. In any case, all the qualitative features of our scenario will be not affected by the uncertainty in the value of N_c.

3. Results

To begin with we show in Fig. 2 the typical mass-radius (MR) relations for the three possible types of compact stars discussed before. The curve labeled with HS represents the MR relation for pure hadronic stars containing an hyperonic core obtained with the GM3 model for the EOS of dense matter. The curve labeled HyS depicts the MR relation for hybrid neutron stars where the hadronic phase is described by the same GM3 model for the EOS and the quark phase by the MIT-bag like model with $B = 136.62$ MeV/fm^3. Finally, if we assume, for example, $B = 69.47$ MeV/fm^3 (with the remaining parameters for quark phase unchanged with respect to the previous case), SQM fulfils the Bodmer-Witten hypothesis and one has the strange star sequence depicted by the curve SS in Fig. 2. As it appears, stars having a deconfined quark content (HyS or SS) are more compact than purely hadronic stars (HS).

In our scenario, we consider a purely hadronic star whose central pressure is increasing due to spin-down or due to mass accretion, *e.g.,* from the material left by the supernova explosion (fallback disc), from a companion star or from the interstellar medium. As the central pressure exceeds the threshold value P_0^* at the static transition point, a virtual drop of quark matter in the Q*-phase can be formed in the central region of the star. As soon as a real drop of Q*-matter is formed, it will grow very rapidly and the original Hadronic Star will be converted to and Hybrid Star or to a Strange Star, depending on the detail of the EOS for quark matter employed to model the phase transition (particularly depending on the value of the parameter B within the model adopted in the present study).

As an illustrative example, we plot in Fig. 3 the potential energy $U(\mathcal{R})$ for the formation of a quark matter droplet for different values of the stellar central pressure P_c above the static transition point P_0^*. The curves in Fig. 3 are relative to a given set of EOS for the two phases

of dense matter (see figure caption), to a fixed value of the surface tension σ and to the case $\gamma = 0$.

As expected the potential barrier is lowered as central pressure increases.

The nucleation time τ, *i.e.,* the time needed to form a critical droplet of deconfined quark matter, can be calculated for different values of the stellar central pressure P_c which enters in the expression of the energy barrier in Eq. (7). The nucleation time can be plotted as a function of the gravitational mass M_{HS} of the HS corresponding to the given value of the central pressure, as implied by the solution of the Tolmann-Oppeneimer-Volkov equations for the pure Hadronic Star sequences. The results of our calculations are reported in Fig. 4 and in Fig. 5 which are relative respectively to the GM1 and GM3 EOS for the hadronic phase. Each curve refers to a different value of the bag constant and the surface tension. As we can see, from the results in Fig.s 4 and 5, a metastable hadronic star can have a mean-life time many orders of magnitude larger than the age of the universe $T_{univ} = (13.7 \pm 0.2) \times 10^9$ yr $= (4.32 \pm 0.06) \times 10^{17}$ s (Spergel et al. 2003). As the star accretes a small amount of mass (of the order of a few per cent of the mass of the sun), the consequential increase of the central pressure lead to a huge reduction of the nucleation time and, as a result, to a dramatic reduction of the HS *mean-life time*.

To summarize, in the present scenario pure hadronic stars having a central pressure larger than the static transition pressure for the formation of the Q*-phase are metastable to the "decay" (conversion) to a more compact stellar configuration in which deconfined quark matter is present (*i.e.,* HyS or SS). These metastable HS have a *mean-life time* which is related to the nucleation time to form the first critical-size drop of deconfined matter in their interior (the actual *mean-life time* of the HS will depend on the mass accretion or on the spin-down rate which modifies the nucleation time via an explicit time dependence of the stellar central pressure). We define as *critical mass* M_{cr} of the metastable HS, the value of the gravitational mass for which the nucleation time is equal to one year: $M_{cr} \equiv M_{HS}(\tau = 1\mathrm{yr})$. Pure hadronic stars with $M_H > M_{cr}$ are very unlikely to be observed. M_{cr} plays the role of an *effective maximum mass* for the hadronic branch of compact stars (see the discussion in subsection 3.1). While the Oppenheimer–Volkov maximum mass $M_{HS,max}$ (Oppenheimer & Volkov 1939) is determined by the overall stiffness of the EOS for hadronic matter, the value of M_{cr} will depend in addition on the bulk properties of the EOS for quark matter and on the properties at the interface between the confined and deconfined phases of matter (*e.g.,* the surface tension σ).

To explore how the outcome of our scenario depends on the details of the stellar matter EOS, we have considered two different parameterizations (GM1 and GM3) for the EOS of the hadronic phase, and we have varied the value of the bag constant B. Moreover,

we have considered two different values for the surface tension: $\sigma = 10$ MeV/fm^2 and $\sigma = 30$ MeV/fm^2 (taking $\gamma = 0$ in both cases). These results are summarized in Tab. 1 (GM1 EOS) and in Tab. 2 (GM3 EOS)

In Fig. 6 and 7, we show the MR curve for pure HS within the GM1 and GM3 models for the EOS of the hadronic phase, and that for hybrid stars or strange stars for different values of the bag constant B. The configuration marked with an asterisk on the hadronic MR curves represents the hadronic star for which the central pressure is equal to P_0^*. The full circle on the hadronic star sequence represents the critical mass configuration, in the case $\sigma = 30$ MeV/fm^2 and $\gamma = 0$. The full circle on the HyS (SS) mass-radius curve represents the hybrid (strange) star which is formed from the conversion of the hadronic star with $M_{HS} = M_{cr}$. We assume (Bombaci & Datta 2000) that during the stellar conversion process the total number of baryons in the star (or in other words the stellar baryonic mass) is conserved. Thus the total energy liberated in the stellar conversion is given by the difference between the gravitational mass of the initial hadronic star ($M_{in} \equiv M_{cr}$) and that of the final hybrid or strange stellar configuration with the same baryonic mass ($M_{fin} \equiv M_{QS}(M_{cr}^b)$):

$$E_{conv} = (M_{in} - M_{fin})c^2 \,. \tag{11}$$

The stellar conversion process, described so far, will start to populate the new branch of quark stars (the part of the QS sequence plotted as a continuous curve in Fig.s 6 and 7). Long term accretion on the QS can next produce stars with masses up to the limiting mass $M_{QS,max}$ for the quark star configurations.

As we can see from the results reported in Tab. 1 and 2, within the present model for the EOS, we can distinguish several ranges for the value of the bag constant, which gives a different astrophysical output for our scenario. To be more specific, in Fig. 8 we plot the maximum mass of the QS sequence, the critical mass and the corresponding final mass M_{fin} as a function of B, in the particular case of the GM3 model for the EOS of the hadronic phase and taking $\sigma = 30$MeV/fm^2 and $\gamma = 0$. Let us start the following discussion from "high" values of B down to the minimum possible value B^V (~ 57.5MeV/fm^3 for $\alpha_s = 0$) for which atomic nuclei will be unstable to the decay to a drop of deconfined *u,d* quark matter (non-strange QM) (Farhi & Jaffe 1984).

(1) $B > B^I$. These "high" values of the bag constant do not allow the quark deconfinement to occur in the maximum mass hadronic star either. Here B^I denotes the value of the bag constant for which the central density of the maximum mass hadronic star is equal to the critical density for the beginning of the mixed quark-hadron phase. For these values of B, all compact stars are pure hadronic stars.

(2) $B^{II} < B < B^I$. Now, in addition to pure HS, there is a new branch of compact

stars, the hybrid stars; but the nucleation time $\tau(M_{HS,max})$ to form a droplet of Q*-matter in the maximum mass hadronic star, is of the same order or much larger than the age of the Universe. Therefore, it is extremely unlikely to populate the hybrid star branch. Once again, the compact star we can observe are, in this case, pure HS.

(3) $B^{III} < B < B^{II}$. In this case, the critical mass for the pure hadronic star sequence is less than the maximum mass for the same stellar sequence, *i.e.,* $M_{cr} < M_{HS,max}$. Nevertheless (for the present EOS model), the baryonic mass $M^b(M_{cr})$ of the hadronic star with the critical mass is larger than the maximum baryonic mass $M^b_{QS,max}$ of the hybrid star sequence. In this case, the formation of a critical size droplet of deconfined matter in the core of the hadronic star with the critical mass, will trigger off a stellar conversion process which will produce, at the end, a black hole (see cases marked as "BH" in Tab. 1 and Tab. 2). As in the previous case, it is extremely unlikely to populate the hybrid star branch. The compact star predicted by these EOS models are pure HS. Hadronic stars with a gravitational mass in the range $M_{HS}(M^b_{QS,max}) < M_{HS} < M_{cr}$ (where $M^b_{QS,max}$ is the baryonic mass of the maximum mass configuration for the hybrid star sequence) are metastable with respect to a conversion to a black hole.

(4) $B^{IV} < B < B^{III}$. For these values of B one has $M_{cr} < M_{HS}(M^b_{QS,max})$. There are now two different branches of compact stars: pure hadronic stars with $M_{HS} < M_{cr}$, and hybrid stars with $M_{QS}(M^b_{cr}) < M_{QS} < M_{QS,max}$ (here $M_{QS}(M^b_{cr}) \equiv M_{fin}$ is the gravitational mass of the hybrid star with the same baryoinic mass of the critical mass hadronic star).

(5) $B^{V} < B < B^{IV}$. Finally, as B falls below the value B^{IV}, the Bodmer-Witten hypothesis starts to be fulfilled. Now the stable quark stars formed in the stellar conversion process are strange stars.

To examine the influence of the curvature energy on the quantum nucleation process, we have performed some calculations of the nucleation time taking $\gamma \neq 0$ in Eq. (7). We have used the two values, $\gamma = 10$ MeV/fm and $\gamma = 20$ MeV/fm, according to the existing estimates of the curvature coefficient in the case of the quark-hadron phase transition (Madsen 1993; Horvath 1994; Olesen & Madsen 1994). As expected, for a fixed value of the stellar central pressure, the curvature term suppresses quark matter nucleation. As a consequence, the critical mass M_{cr} and the total energy released in the stellar conversion process are increasesd with respect to the case $\gamma = 0$, as it can be seen looking at the results reported in Tab. 3.

3.1. The limiting mass of compact stars

The possibility to have metastable hadronic stars, together with the feasible existence of two distinct families of compact stars, demands an extension of the concept of maximum mass of a "neutron star" with respect to the *classical* one introduced by Oppenheimer & Volkoff (1939). Since metastable HS with a "short" *mean-life time* are very unlikely to be observed, the extended concept of maximum mass must be introduced in view of the comparison with the values of the mass of compact stars deduced from direct astrophysical observation. Having in mind this operational definition, we call *limiting mass* of a compact star, and denote it as M_{lim}, the physical quantity defined in the following way:

(a) if the nucleation time $\tau(M_{HS,max})$ associated to the maximum mass configuration for the hadronic star sequence is of the same order or much larger than the age of the universe T_{univ}, then

$$M_{lim} = M_{HS,max} \, , \tag{12}$$

in other words, the limiting mass in this case coincides with the Oppenheimer–Volkoff maximum mass for the hadronic star sequence.

(b) If the critical mass M_{cr} is smaller than $M_{HS,max}$ (*i.e.* $\tau(M_{HS,max}) < 1$ yr), thus the limiting mass for compact stars is equal to the largest value between the critical mass for the HS and the maximum mass for the quark star (HyS or SS) sequence

$$M_{lim} = max[M_{cr} \, , M_{QS,max}] \, . \tag{13}$$

(c) Finally, one must consider an "intermediate" situation for which 1yr $< \tau(M_{HS,max}) < T_{univ}$. As the reader can easely realize, now

$$M_{lim} = max[M_{HS,max} \, , M_{QS,max}] \, , \tag{14}$$

depending on the details of the EOS which could give $M_{HS,max} > M_{QS,max}$ or vice versa.

In Fig. 9, we show the limiting mass M_{lim} calculated in the case of the GM1+Bag model (dashed line) and in the case of the GM3+Bag model (continuous line) as a function of the bag constant B. In the same figure, we compare our theoretical determination for M_{lim} with some of the "measured" masses of compact stars in radio pulsar binaries (Thorsett & Chakrabarty 1999) and for the compact stars Vela X-1 (Quaintrell et al. 2003) and Cygnus X-2 (Orosz & Kuulkers 1999).

4. Mass-to-radius ratio and internal constitution of compact stars

An accurate measure of the radius and the mass of an individual "neutron star" will represent the key to open the *safety deposit* which contains the secrets of the internal constitution of these puzzling astrophysical bodies and to discriminate between different models for the equation of state of dense hadronic matter. Unfortunately such a crucial information is still not available. A decisive step in such a direction has been done thanks to the instruments on board of the last generation of X-ray satellites. These are providing a large amount of fresh and accurate observational data, which are giving us the possibility to extract very tight constraints on the radius and the mass for some compact stars.

The analysis of different astrophysical phenomena associated with compact X-ray sources, seems to indicate in some case the existence of neutron stars with "large" radii in the range of 12 – 20 km and in some other cases the existence of compact stars with "small" radii in the range of 6 – 9 km (Bombaci 1997; Li et al. 1999a; Poutanen & Gierlinski 2003; Bombaci 2003). Clearly, this possibility is a natural outcome of our scenario, where two different families of compact stars, the pure hadronic stars and the quark stars (HyS or SS), may exist in the universe.

In the following of this section, we will consider some of the most recent constraints on the mass-to-radius ratio for compact stars extracted from the observational data for a few X-ray sources, and we will try make an interpretation of these results within our scenario.

In Fig. 10, we report the radius an the mass of the compact star RX J1856.5-3754 inferred by Walter & Lattimer (2002) (see also Kaplan et al. 2002) from the fit of the full spectral energy distribution for this isolated radio-quite "neutron star", after a revised parallax determination (Kaplan et al. 2002) which implies a distance to the source of 117 ± 12 pc. Comparing the mass-radius box for RX J1856.5-3754 reported in Fig. 10 with the theoretical determination of the MR relation for different equations of state, one concludes that RX J1856.5-3754 could be (see *e.g.* Fig. 2 in Walter & Lattimer, 2002) either an hadronic star or an hybrid or strange star (see also Drake et al. 2002).

Next we consider the compact star in the low mass X-ray binary 4U 1728-34. In a very recent paper Shaposhnikov et al. (2003) (hereafter STH) have analyzed a set of 26 Type-I X-ray bursts for this source. The data were collected by the Proportional Counter Array on board of the Rossi X-ray Timing Explorer (RXTE) satellite. For the interpretation of these observational data Shaposhnikov et al. 2003 used a model of the X-ray burst spectral formation developed by Titarchuk (1994) and Shaposhnikov & Titarchuk 2002. Within this model, STH were able to extract very stringent constrain on the radius and the mass of the compact star in this bursting source. The radius and mass for 4U 1728-34, extracted by STH

for different best-fits of the burst data, are depicted in Fig. 10 by the filled squares. Each of the four MR points is relative to a different value of the distance to the source (d = 4.0, 4.25, 4.50, 4.75 kpc, for the fit which produces the smallest values of the mass, up to the one which gives the largest mass). The error bars on each point represent the error contour for 90% confidence level. It has been pointed out (Bombaci 2003) that the semi-empirical MR relation for the compact star in 4U 1728-34 obtained by STH is not compatible with models pure hadronic stars, while it is consistent with strange stars or hybrid stars.

Assuming RX J1856.5-3754 to be a pure hadronic star and 4U 1728-34 an hybrid or a strange star, we see from our results plotted in Fig. 10, that this possibility can be realized as a natural consequence of our scenario. Thus, we find that the existence of quark stars (with "small" radii) does not exclude the possible existence of pure hadronic stars (with "large" radii), and *vice versa*.

Decisive informations on the mass-to-radius ratio can be provided by measuring the gravitational redshift of lines in the spectrum emitted from the compact star atmosphere. Very recently, redshifted spectral lines features have been reported for two different X-ray sources (Cottam et al. 2002; Sanwal et al. 2002). The first of these sources is the compact star in the low mass X-ray binary EXO 0748-676. Studing the spectra of 28 type-I X-ray bursts in EXO 0748-676, Cottam et al. (2002) have found absorption spectral line features, which they identify as signatures of Fe XXVI (25-time ionized hydrogen-like Fe) and Fe XXV from the $n = 2 \rightarrow 3$ atomic transition, and of O VIII ($n = 1 \rightarrow 2$ transition). All of these lines are redshifted, with a unique value of the redshift $z = 0.35$. Interpreting the measured redshift as due to the strong gravitational field at the surface of the compact star (thus neglecting general relativistic effects due to stellar rotation on the spectral lines (Öezel & Psaltis 2003)), one obtains a relation for the stellar mass-to-radius ratio:

$$M/M_{\odot} = \Big(1 - \frac{1}{(z+1)^2}\Big) R/R_{g\odot} \,, \tag{15}$$

($R_{g\odot} = 2GM_{\odot}/c^2 = 2.953$ km) which is reported in Fig.s 6 and 7 as a dashed line labeled $z = 0.35$. Comparing with the theoretical MR relations for differente EOS (see e.g. Fig. 6,, and also Xu 2003) it is clear that all three possible families of compact stars discussed in the present paper are completely consistent with a redshitf $z = 0.35$.

The second source for which it has been claimed the detection of redshifted spectral lines is 1E 1207.4-5209, a radio-quite compact star located in the center of the supernova remnant PSK 1209-51/52. 1E 1207.4-5209 has been observed by the Chandra X-ray observatory. Two absorption features have been detected in the source spectrum and have been interpreted (Sanwal et al. 2002) as spectral lines associated with atomic transitions of once-ionized helium in the atmosphere of a strong magnetized ($B \sim 1.5 \times 10^{14}$ G) compact star. This

interpretation gives for the gravitational redshift at the star surface $z = 0.12 – 0.23$ (Sanwal et al. 2002), which is reported in Fig.s 6 and 7 by the two dashed lines labeled $z = 0.12$ and $z = 0.23$.

A different interpretation of similar data, collected by the XMM-Newton satellite, has been recently given by Bignami et al. (2003), who interpreted the absorption features in the spectrum of 1E 1207.4-5209 as electron cyclotron lines in the stellar magnetic field. Within this interpretation and assuming the gravitational redshift of a "canonical neutron star" with $M = 1.4 M_\odot$ and $R = 10$ km Bignami et al. (2003) derived a magnetic field strength $B = 8 \times 10^{10}$ G for the compact star in 1E 1207.4-5209 .

The two values of the stellar magnetic field inferred in the above quoted papers (Sanwal et al. 2002; Bignami et al. 2003) are in disagreement to each other and in disagreement with the B field deduced from the 1E 1207.4-5209 timing parameters (P and $\dot{P}$), which give $B = (2 – 3) \times 10^{12}$ G within the rotating magnetic dipole model. However, the latter value of the magnetic field strenght presents serious problems since the current values of the timing parameters implies a characteristic pulsar age $\tau_c = P/(2\dot{P}) \sim 4.8 \times 10^5$ yr (Bignami et al. 2003) which is not compatible with the age $\tau_{SNR} = (3–20) \times 10^3$ yr (Roger et al. 1988). Clearly this source needs a more accurate study before any final and unambiguous interpretations of the observed spectral features can be drawn. Here, we will assume that the interpretation of the spectral feature given by Sanwal et al. (2002) and by Cottam et al. (2002) is correct. In that case, how it is possible to reconcile the gravitational redshift $z =$012–0.23 for 1E 1207.4-5209 with that ($z = 0.35$) deduced for EXO 0748-676? Within the commonly accepted view, in which there exist in nature only one family of compact stars (the "neutron stars"), different values of the gravitational redshift could be a consequence of a different mass of the two stars. In our scenario, we can give a different interepretation: 1E 1207.4-5209 is a pure hadronic star whereas EXO 0748-676 is an hybrid star or a strange star. This is illustrated in Fig.s 6 and 7 by comparing our calculated MR relations with the redshifts deduced for the two compact X-ray sources.

5. Quark Deconfinement Nova and GRBs

A large variety of observational data are giving a mounting evidence that "long-duration" Gamma Ray Bursts (GRBs) are associated with supernova explosions (Bloom et al. 1999; Amati et al. 2000; Antonelli et al. 2000; Piro et al. 2000, Reeves et al. 2002; Hjorth et al. 2003; Price et al. 2003; Stanek et al. 2003; Lipkin et al. 2003). Particularly, in the case of the gamma ray burst of July 5, 1999 (GRB990705), in the case of GRB020813 and of GRB011211, it has been possible to estimate the time delay between the two events.

For GRB990705 Amati et al. (2000) evaluated that the supernova explosion (SNE) has occurred about 10 years before the GRB, while Lazzati et al. (2001), giving a different interpretation of the same observational data, deduced a time delay of about one year. In the case of GRB020813 the supernova event has been estimated (Butler et al. 2003) to have occurred a few months before the GRB, while in the case of GRB011211 about four days before the burst (Reeves et al. 2002). If a time-delay between a SNE and the associated GRB will be confirmed by further and more accurate observations, thus it is necessary to have a two-step process. The first of these process is the supernova explosion which forms a compact stellar remnant, *i.e.* a neutron star. The second catastrophic event is associated with the neutron star and it is the energy source for the observed GRB. These new observational data, and the two-step scenario outlined above, poses severe problems for most of the current theoretical models for the central energy source (the so called "central engine") of GRBs.

In a recent paper Berezhiani et al. (2003) have given a simple and natural interpretation of the "delayed" Supernova-GRB connection in terms of the stellar conversion model (hereafter the *Quark Deconfinement Nova* (QDN)) discussed in the present work. Here, with respect to the work of Berezhiani et al. (2003), we have considered two different parameterizations (GM1 and GM3) for the EOS of the hadronic phase, and we have explored a larger range for the bag constant in the EOS for the quark phase. Moreover, in the present paper the nucleation time has been calculated by considering the quantum tunneling of a virtual drop of quark matter in the so called Q*-phase (see sect. 2), contrary to the work of Berezhiani et al. (2003) where quark flavor conservation during the deconfinement transition has been neglected. We have verified that flavor conservation in computing the nucleation time produces sizable differences in the value of the critical mass M_{cr} and on the energy released during the QDN which powers the GRB.

As we can see from the results reported in Tab.s 1 and 2, the total energy (E_{conv}) liberated during the stellar conversion process is in the range 0.5–1.7$\times 10^{53}$ erg. This huge amount of energy will be mainly carried out by the neutrinos produced during the stellar conversion process. It has been pointed out by Salmonson & Wilson (1999) that near the surface of a compact stellar object, due to general relativity effects, the efficiency of the neutrino-antineutrino annihilation into e^+e^- pairs is strongly enhanced with respect to the Newtonian case, and it could be as high as 10%. The total energy deposited into the electron-photon plasma can therefore be of the order of 10^{51}–10^{52} erg.

The strong magnetic field of the compact star will affect the motion of the electrons and positrons, and in turn could generate an anisotropic γ-ray emission along the stellar magnetic axis. This picture is strongly supported by the analysis of the early optical afterglow for

GRB990123 and GRB021211 (Zhang et al. 2003), and by the recent discovery of an ultra-relativistic outflow from a "neutron star" in a binary stellar system (Fender et al. 2004). Moreover, it has been recently shown (Lugones et al. 2002) that the stellar magnetic field could influence the velocity of the "burning front" of hadronic matter into quark matter. This results in a strong geometrical asymmetry of the forming quark matter core along the direction of the stellar magnetic axis, thus providing a suitable mechanism to produce a collimated GRB (Lugones et al. 2002). Other anisotropies in the GRB could be generated by the rotation of the star.

6. Summary

In the present work, we have investigated the consequences of the hadron-quark deconfinement phase transition in stellar compact objects when finite size effects between the deconfined quark phase and the hadronic phase are taken into account. We have found that above a threshold value of the gravitational mass a pure hadronic star is metastable to the decay (conversion) to a hybrid neutron star or to a strange star [1]. We have calculated the *mean-life time* of these metastable stellar configurations, the critical mass for the hadronic star sequence, and have explored how these quantities depend on the details of the EOS for dense matter. We have introduced an extension of the concept of limiting mass of compact stars, with respect to the classical one given by Oppenheimer & Volkov (1939). We have demonstrated that, within the astrophysical scenario proposed in the present work, the existence of compact stars with "small" radii (quark stars) does not exclude the existence of compact stars with "large" radii (pure hadronic stars), and *vice versa*.

Finally, we have shown that our scenario implies, as a natural consequence a two step-process which is able to explain the inferred "delayed" connection between supernova explosions and GRBs, giving also the correct energy to power GRBs.

There are various specific features and predictions of the present model, which we briefly mention in the following. The second explosion (*Quark Deconfinement Nova*) take place in a "baryon-clean" enviroment due to the previous SN explosion. Is is possible to have different time delays between the two events since the *mean-life time* of the metastable hadronic star

[1] The particular type of quark star (it i.e. hybrid star or strange star) formed at the end of the stellar conversion, will depend on the details of the quark matter EOS (see sect. 3). Here we want to stress that our scenario does not require as a necessary condition the fulfilment of the Bodmer-Witten hypothesis on the absolute stability of strange matter and, thus the existence of strange stars. The delayed stellar conversion process described in this paper takes place also in the case a more "traditional" hybrid star is formed.

depends on the value of the stellar central pressure. Thus the present model is able to interpret a time delay of a few years (as observed in GRB990705 (Amati et al. 2000; Lazzati et al. 2001)), of a few months (as in the case of GRB020813 (Butler et al. 2003)), of a few days (as deduced for GRB011211 (Reeves et al. 2002)), or the nearly simultaneity of the two events (as in the case of SN2003dh and GRB030329 (Hjorth et al. 2003)).

It is a pleasure to acknowledge stimulating discussions with David Blaschke, Alessandro Drago, Bennett Link, German Lugones, and Sergei B. Popov.

REFERENCES

Alcock, C., Farhi, E., & Olinto, A. 1986, ApJ, 310, 261

Amati, L. et al., 2000, Science, 290, 953

Antonelli, L.A. et al. 2000, ApJ, 545, L39

Baym, G., & Chin, S.A. 1976, Phys. Lett. B, 62, 241

Benvenuto, O.G., & Horvath, J.E. 1998, Phys. Rev. Lett. , 63, 716

Berezhiani, Z., Bombaci, I., Drago, A., Frontera, F., & Lavagno, A. 2003, ApJ, 586, 1250

Bignami, G.F., Carvero, P.A., De Luca, A., & Mereghetti, S., 2003, Nature, 423, 725

Bloom, J.S. et al. 1999, Nature, 401, 453

Bodmer, A.R. 1971, Phys. Rev. D, 4, 1601

Bombaci, I., 1996, A &A , 305, 871

Bombaci, I., 1997, Phys. Rev. C, 55, 1587

Bombaci, I., 2003, astro-ph/0307522

Bombaci, I., et al. 2004, work in progress

Bombaci, I., & Datta, B. 2000, ApJ, 530, L69

Butler, N.R., et al. 2003, ApJ, 597, 1010

Cheng, K.S., Dai, Z.G., Wai, D.M., & Lu, T., 1998, Science, 280, 407

Collins, J.C., & Perry, M.J. 1975, Phys. Rev. Lett., 34, 1353

Cottam, J., Paerels, F., & Mendez, M. 2002, Nature, 420, 51

Dey, M., Bombaci, I., Dey, J., Ray, S., & Samanta, B.C. 1998, Phys. Lett. B, 438, 123; erratum 1999, Phys. Lett. B, 467, 303

Drago, A., & Lavagno, A. 2001, Phys. Lett. B, 511, 229

Drake, J.J., et al. 2002, ApJ, 572, 996

Farhi, E., & Jaffe, R.L. 1984, Phys. Rev. D, 30, 2379

Fender, R., et al. 2004, Nature, 427, 222

Grassi, F. 1998, ApJ, 492, 263

Glendenning, N.K 1992, Phys. Rev. D, 46, 1274

Glendenning, N.K., 1996, Compact Stars: Nuclear Physics, Particle Physics, and General Relativity, Springer Verlag

Glendenning, N.K., & Moszkowski, S.A. 1991, Phys. Rev. Lett., 67, 2414

Haensel, P., Zdunik, J.L. & Schaefer, R. 1986, A&A, 160, 121

Haensel, P. 2003, Equation of state of dense matter and maximum mass of neutron stars, in Final Stages of Stellar Evolution, Ed. C. Motch and J.-M. Hameury, EAS Publications Series 7, 249

Heiselberg, H., Pethick, C.J., & Staubo, E.F. 1993, Phys. Rev. Lett., 70, 1355

Heiselberg, H. 1995, in Strangeness and Quark Matter, World Scientific, 338

Hjorth, J. et al, 2003, Nature, 423, 847

Horvath, J.E., Benvenuto, O.G., & Vucetich, H. 1992, Phys. Rev. D, 45, 3865

Horvath, J.E. 1994, Phys. Rev. D, 49, 5590

Iachello, F., Langer, W.D., & Lande, A. 1974, Nucl. Phys. A, 219, 612

Iida, K., & Sato, K. 1997, Prog. Theor. Phys., 1, 277: 1998, Phys. Rev. C, 58, 2538

Itoh, N. 1970, Prog. Theor. Phys., 44, 291

Ivanenko, D., & Kurdgelaidze, D.F. 1969, Lett. Nuovo Cimento, 2, 13

Kaplan, D.L., van Kerkwijk, M.H, & Anderson, J. 2002, ApJ, 571, 447

Keister, B.D., & Kisslinger, L.S., 1976, Phys. Lett. B, 64, 117

Lazzati, D., Ghisellini, G., Amati, L., Frontera, F., Vietri, M., & Stella, L. 2001, ApJ, 556, 471

Li, X.–D., Bombaci, I., Dey, M., Dey J., & van den Heuvel, E.P.J. 1999a, Phys. Rev. Lett., 83, 3776

Li, X.–D., Ray, S., Dey, J., Dey, M., & Bombaci, I. 1999b, ApJ, 527, L51

Lifshitz, I. M., & Kagan, Y. 1972, Sov. Phys. JETP, 35, 206

Lipkin, Y.M. 2003, astro-ph/0312594

Lugones, G., & Benvenuto, O.G. 1998 , Phys. Rev. D, 58, 083001

Lugones, G., Ghezzi, C.R., de Gouveia Dal Pino E.M., & Horvath, J.E. 2002, ApJ, 581, L101

Madsen, J. 1993, Phys. Rev. Lett., 70, 391

Madsen, J. 1999, Lectures Notes in Physics Vol. 500, Springer Verlag, 162

Müller, H., & Serot, B.D. 1995, Phys. Rev. C, 52, 2072

Olesen, M.L., & Madsen, J. 1994, Phys. Rev. D, 49, 2698

Oppenheimer, J.R., & Volkoff, G.M. 1939, Phys. Rev., 55, 374

Orosz, J.A., & Kuulkers, E. 1999, MNRAS, 305, 132

Özel, F. & Psaltis, D. 2003, ApJ, 582, L31

Piro, L. et al. 2000, Science, 290, 955

Poutanen, J. & Gierliǹski, M. 2003, MNRAS, 343, 1301

Prakash, M., Bombaci, I., Prakash, M., Ellis, P.J., Lattimer, J.M., & Knorren, R. 1997, Phys. Rep. 280, 1

Price, P.A. et al. 2003, Nature, 423, 844

Quaintrell, H., et al., 2003, A&A, 401, 313

Reeves, J.N. et al., 2002, Nature, 414, 512

Roget, R.S., Milne, D.K., Kesteven, M.J., Wellington, K.J., & Haynes, R.F. 1988, ApJ, 332, 940

Salmonson, J.D., & Wilson, J.R. 1999, ApJ, 517, 859

Sanwal, D., Pavlov, G.G., Zavlin, V.E., & Teter, M.A. 2002, ApJ, 574, L61

Shapiro, S.L. & Teukolsky, S.A. 1983, Black holes, white dwarfs and neutron stars, Ed. J. Wiley& Sons

Shaposhnikov, N. , & Titarchuk, L. 2002, ApJ, 570, L25

Shaposhnikov, N. , Titarchuk, L., & Haberl, F. 2003, ApJ, 593, L38 (STH)

Spergel, D.N. 2003, Astrophys. J. Suppl., 148, 175

Stanek, K.Z. et al. 2003, ApJ, 591, L17

Terazawa, H. 1979, INS-Report, 336 (INS, Univ. of Tokyo); 1989, J. Phys. Soc. Japan, 58, 3555; 1989, J. Phys. Soc. Japan, 58, 4388

Thorsett, S.E., & Chakrabarty D. 1999, ApJ, 512, 288

Titarchuk, L. 1994, ApJ, 429, 330

van Kerkwijk, M.H. *et al.*1995, A&A 303, 483

Voskresensky, D.N., Yasuhira, M, & Tatsumi, T. 2003, Nucl. Phys. A, 723, 291

Walter, F.M., & Lattimer, J.M. 2002, ApJ, 576, L148

Witten, E. 1984, Phys. Rev. D, 30, 272

Xu, R.X. 2002, ApJ, 570, L65

Xu, R.X. 2003, Chin. J. Astron. Astrophys., 3, 33

Zhang, B., Kobayashi, S., & Meszaros, P. 2003, ApJ, 595, 950

Table 1: Critical masses and energy released in the conversion process of an HS into a QS for several values of the Bag constant and the surface tension. Column labelled $M_{QS,max}$ ($M^b_{QS,max}$) denotes the maximum gravitational (baryonic) mass of the final QS sequence. The value of the critical gravitational (baryonic) mass of the initial HS is reported on column labelled M_{cr} (M^b_{cr}) whereas those of the mass of the final QS and the energy released in the stellar conversion process are shown on columns lallebed M_{fin} and E_{conv} respectively. BH denotes those cases in which due to the conversion the initial HS collapses into a black hole. Units of B and σ are MeV/fm^3 and MeV/fm^2 respectively. All masses are given in solar mass units and the energy released is given in units of 10^{51} erg. The hadronic phase is described with the GM1 model, m_s and α_s are always taken equal to 150 MeV and 0 respectively. The GM1 model preditcs a maximum mass for the pure HS of 1.807 $M_\odot$.

			$\sigma = 10$				$\sigma = 30$			
B	$M_{QS,max}$	$M^b_{QS,max}$	M_{cr}	M^b_{cr}	M_{fin}	E_{conv}	M_{cr}	M^b_{cr}	M_{fin}	E_{conv}
208.24	1.769	2.002	1.798	2.040	BH		1.805	2.050	BH	
169.61	1.633	1.828	1.754	1.983	BH		1.778	2.014	BH	
136.63	1.415	1.561	1.668	1.871	BH		1.719	1.937	BH	
108.70	1.426	1.604	1.510	1.673	BH		1.615	1.804	BH	
106.17	1.433	1.617	1.490	1.649	BH		1.602	1.788	BH	
103.68	1.441	1.632	1.469	1.623	1.434	62.5	1.588	1.770	BH	
101.23	1.449	1.648	1.447	1.596	1.411	64.0	1.574	1.752	BH	
98.83	1.459	1.665	1.425	1.569	1.388	66.0	1.559	1.734	BH	
96.47	1.470	1.684	1.402	1.541	1.364	68.5	1.543	1.715	BH	
94.15	1.481	1.704	1.378	1.513	1.339	71.1	1.527	1.694	1.474	94.8
91.87	1.494	1.726	1.354	1.484	1.313	74.2	1.511	1.674	1.456	98.1
89.64	1.507	1.750	1.329	1.453	1.285	77.3	1.495	1.654	1.438	101.8
87.45	1.552	1.776	1.302	1.422	1.257	80.7	1.477	1.632	1.417	105.9
85.29	1.538	1.803	1.275	1.389	1.228	84.4	1.458	1.610	1.397	110.4
80.09	1.581	1.879	1.196	1.296	1.144	92.9	1.410	1.551	1.342	122.7
75.12	1.631	1.966	1.082	1.164	1.029	93.78	1.359	1.489	1.284	133.1
65.89	1.734	2.156	0.820	0.867	0.764	100.6	1.212	1.315	1.123	159.9
63.12	1.770	2.222	0.727	0.764	0.672	98.1	1.160	1.254	1.067	166.5
59.95	1.814	2.305	0.545	0.566	0.501	79.7	1.081	1.162	0.986	168.8

Table 2: Same as Table 1 for the GM3+Bag model. The situations for which there is no deconfinement phase transition, or for wich the nucleation time of the hadronic maximum mass configuration is of the order or larger that the age of the universe (see discusion in the text) are reported with no entry (-) The maximum mass for the pure HS predicted by the GM3 model is 1.552 $M_\odot$.

			$\sigma = 10$				$\sigma = 30$			
B	$M_{QS,max}$	$M^b_{QS,max}$	M_{cr}	M^b_{cr}	M_{fin}	E_{conv}	M_{cr}	M^b_{cr}	M_{fin}	E_{conv}
136.63	1.448	1.613	-	-	-		1.551	1.734	BH	
122.07	1.430	1.600	-	-	-		1.539	1.718	BH	
108.70	1.440	1.627	1.484	1.648	BH		1.498	1.665	BH	
106.17	1.445	1.637	1.474	1.635	1.444	53.4	1.487	1.651	BH	
103.68	1.451	1.648	1.461	1.619	1.430	56.2	1.475	1.636	1.442	57.9
101.23	1.458	1.661	1.449	1.603	1.415	59.3	1.462	1.620	1.428	60.9
98.83	1.466	1.676	1.435	1.587	1.400	62.5	1.449	1.604	1.413	64.3
96.47	1.475	1.692	1.421	1.569	1.384	66.3	1.436	1.587	1.398	68.0
94.15	1.485	1.710	1.406	1.550	1.367	70.0	1.422	1.570	1.382	71.9
91.87	1.497	1.731	1.390	1.531	1.348	74.2	1.407	1.552	1.365	76.2
89.64	1.509	1.753	1.373	1.510	1.329	78.5	1.392	1.534	1.347	80.8
87.45	1.523	1.778	1.355	1.488	1.308	83.1	1.376	1.515	1.329	85.7
85.29	1.538	1.804	1.335	1.463	1.285	87.8	1.360	1.495	1.310	90.6
80.09	1.582	1.881	1.270	1.385	1.214	98.7	1.314	1.438	1.255	104.0
75.12	1.631	1.966	1.181	1.280	1.121	107.8	1.252	1.365	1.187	116.85
65.89	1.734	2.155	0.943	1.005	0.877	117.8	1.126	1.216	1.045	144.5
63.12	1.770	2.222	0.808	0.854	0.747	110.2	1.082	1.164	0.997	152.1
59.95	1.814	2.305	0.513	0.531	0.471	74.7	1.010	1.081	0.923	155.5

Table 3: Critical masses and energy released in the conversion process of an HS into a QS for several values of the curvature coefficient γ. The results are realtive to the GM1 model for the hadronic phase. For the quark phase we take $B = 75.12$ MeV/fm^3, $m_s = 150$ MeV and $\alpha_s = 0$. The surface tension is $\sigma = 30$ MeV/fm^2. All the quantities reported in the table have the same units as in Tab. 1.

γ	M_{cr}	M_{cr}^b	M_{fin}	E_{conv}
0	1.359	1.489	1.284	133.1
10	1.390	1.526	1.313	137.9
20	1.418	1.561	1.338	142.3

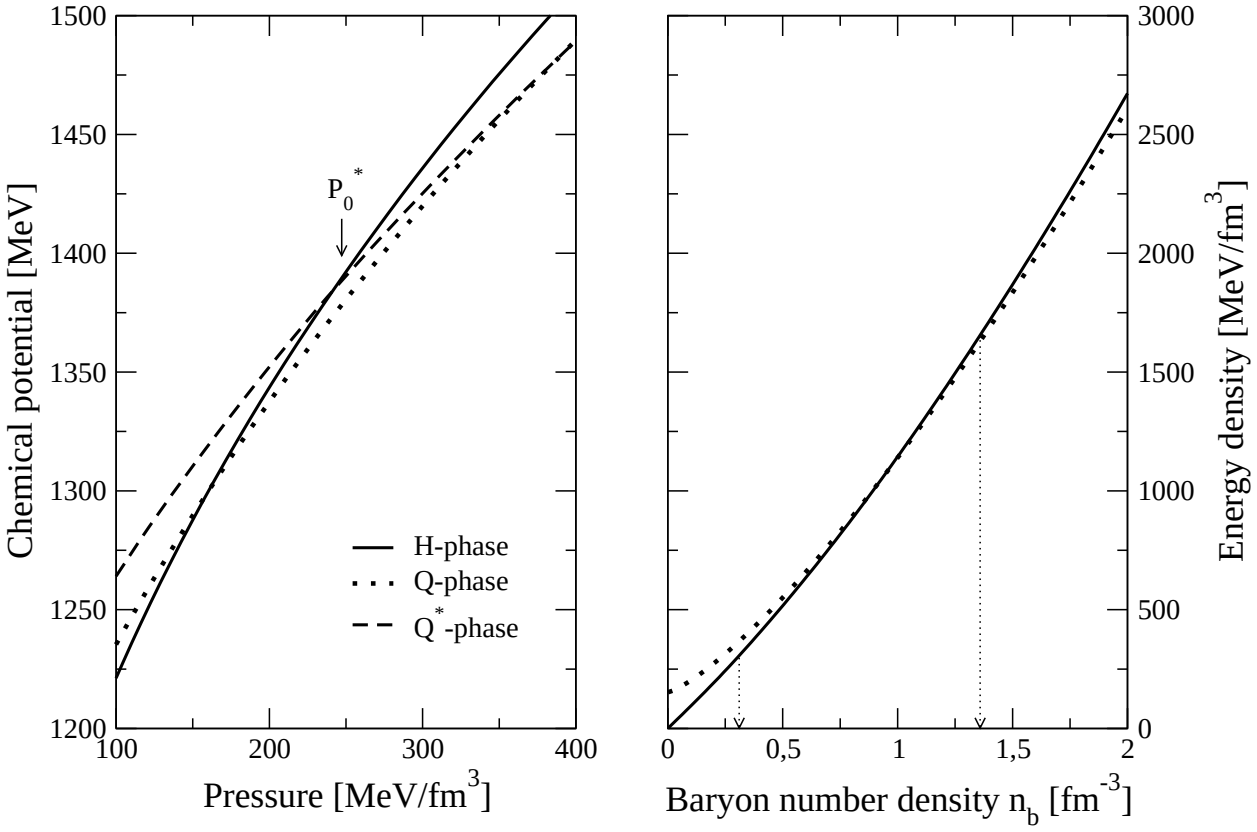

Fig. 1.— Chemical potentials of the three phases of matter (H, Q, and Q*), as defined by Eq. (2) as a function of the total pressure (left panel); and energy density of the H- and Q-phase as a function of the baryon number density (right panel). The hadronic phase is described with the GM3 model whereas for the Q and Q* phases is employed the MIT-like bag model with $m_s = 150$ MeV, $B = 152.45$ MeV/fm^3 and $\alpha_s = 0$. The vertical lines arrows on the right panel indicate the beginning and the end of the mixed hadron-quark phase defined according to the Gibbs criterion for phase equilibrium. On the left panel P_0^* denotes the static transition point.

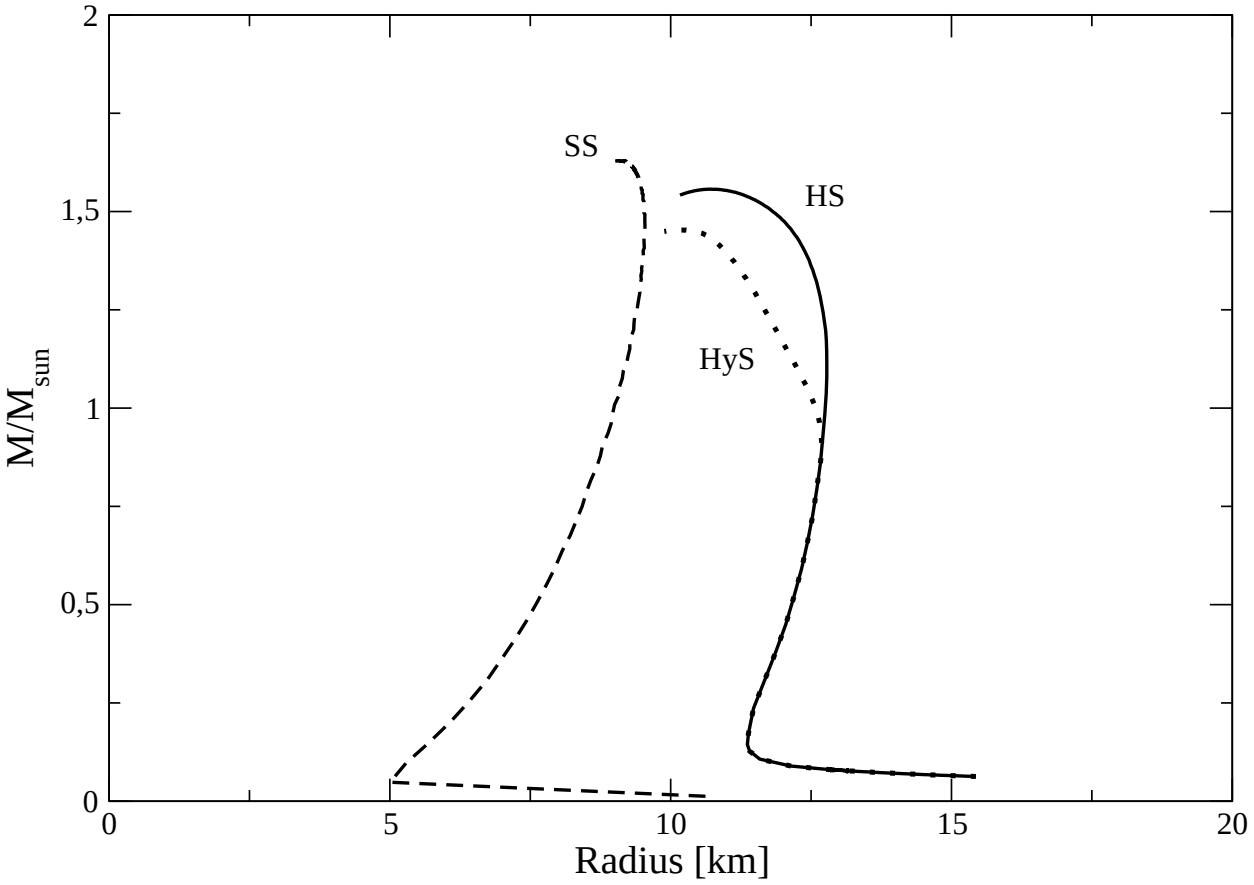

Fig. 2.— Mass-radius relations for the three types of compact objects discussed in the text: Hadronic Star (HS), Hybrid Star (HyS) and Strange Star (SS). The hadronic phase is described with the GM3 model while the pure quark phase is described by the MIT-like bag model with $m_u = m_d = 0$, $m_s = 150$ MeV, $\alpha_s = 0$ and $B = 136.62(69.47)$ MeV/fm^3 for the hybrid star (strange star).

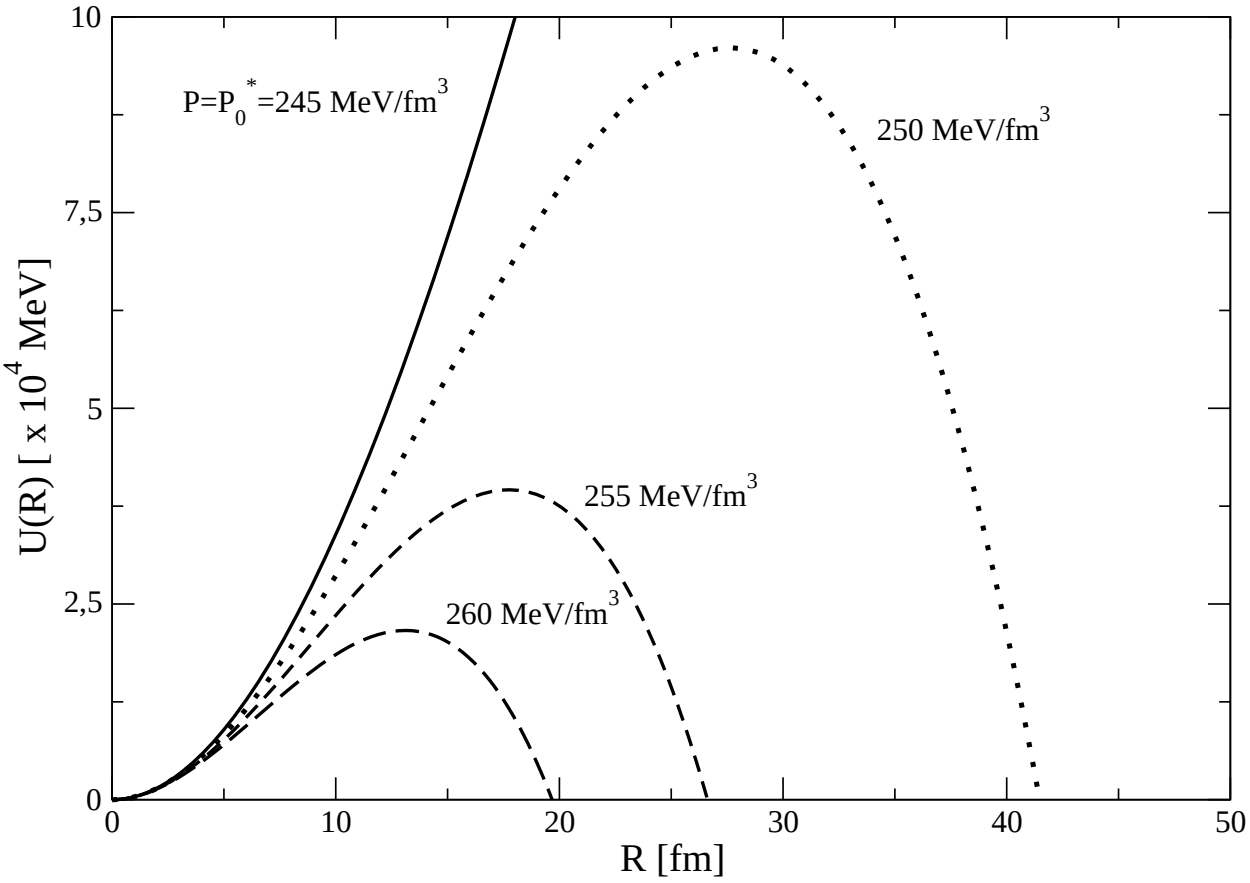

Fig. 3.— Potential energy of the QM drop as a function of the radius of the drop for several pressures above P_0^*. The hadronic and Q* phases are described with the same EoS employed in Fig. 1. The surface tension σ is taken equal to 30 MeV/fm^2 and the curvature coefficient γ is taken equal to zero.

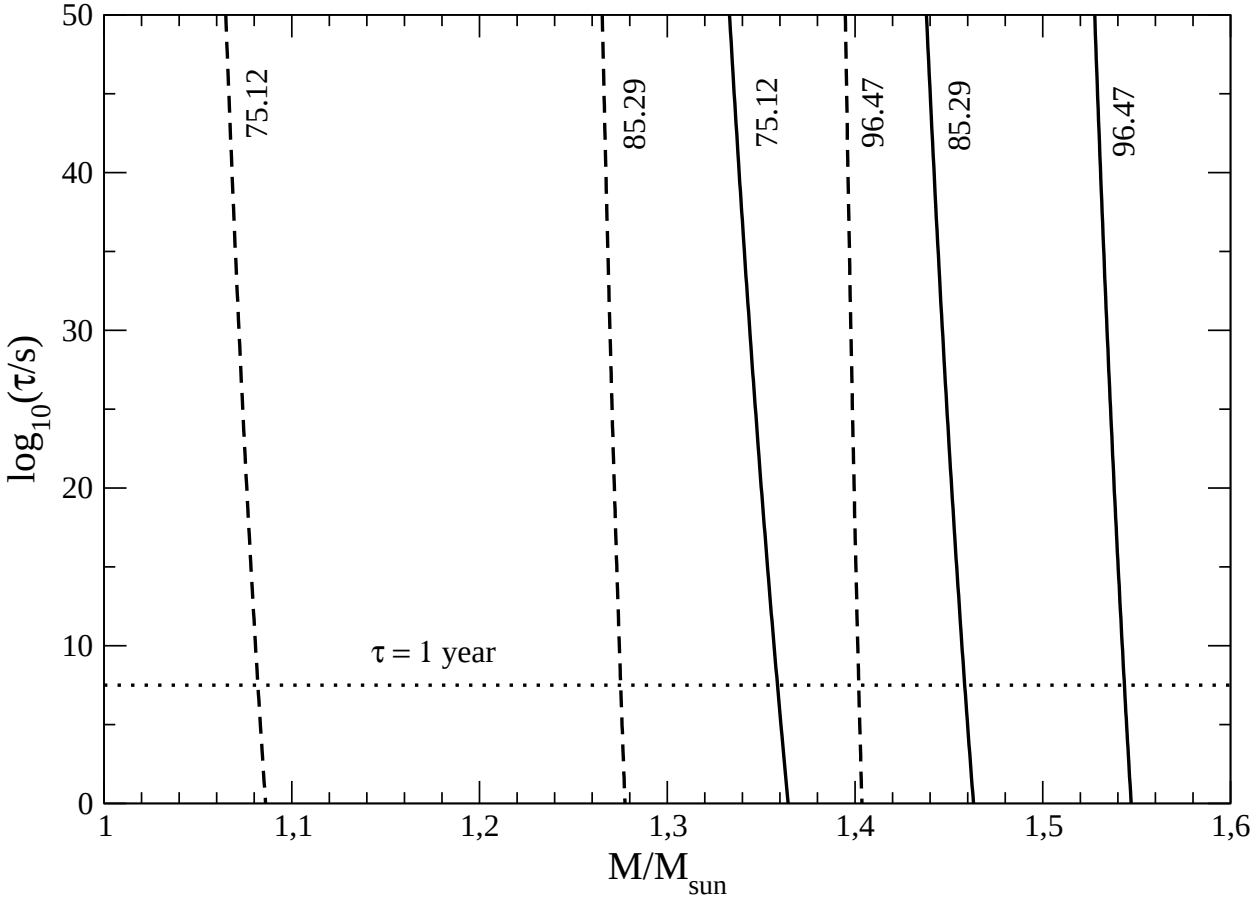

Fig. 4.— Nucleation time as a function of the maximum gravitational mass of the hadronic star. Solid lines correspond to a value of $\sigma = 30$ MeV/fm^2 whereas dashed ones are for $\sigma = 10$ MeV/fm^2. In both cases we take $\gamma = 0$. The nucleation time correspondig to one year is shown by the dotted horizontal line. The different values of the bag constant (in units of MeV/fm^3) are plotted next to each curve. The hadronic phase is described with the GM1 model.

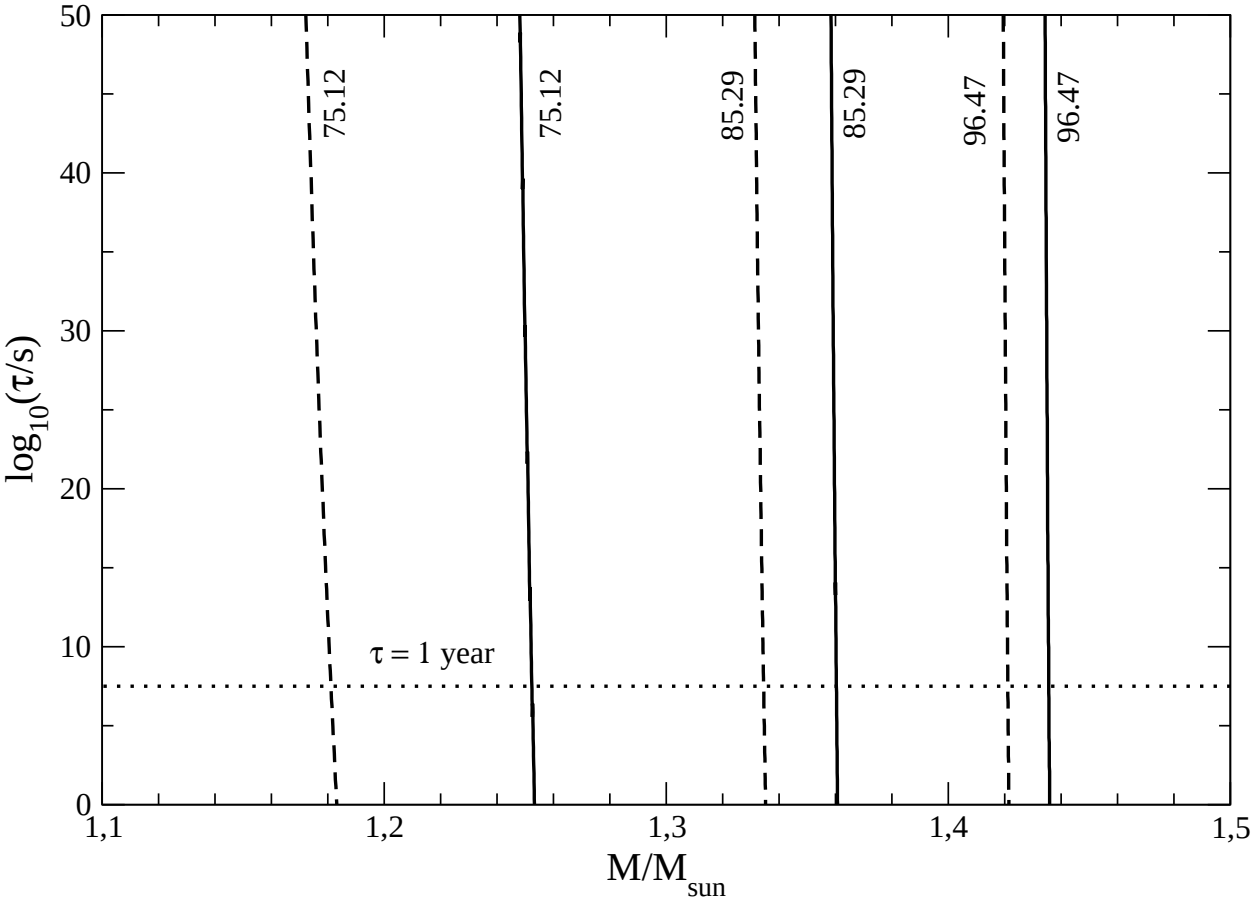

Fig. 5.— Same as Fig. 4 for the GM3+Bag model.

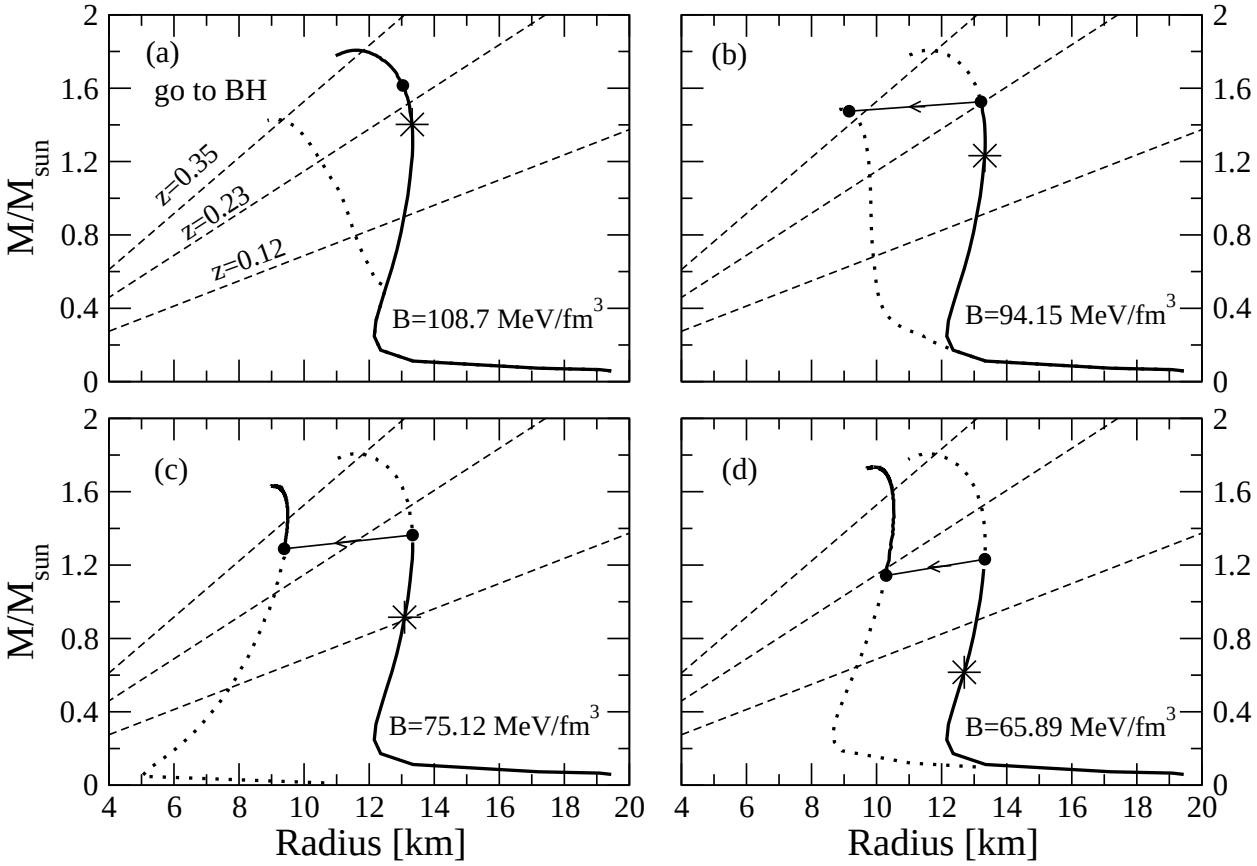

Fig. 6.— Mass-radius relation for a pure HS described within the GM1 model and that of the HyS or SS configurations for several values of the Bag constant and $m_s = 150$ MeV and $\alpha_s = 0$. The configuration marked with an asterisk represents in all cases the HS for which the central pressure is equal to P_0^*. The conversion process of the HS, with a gravitational mass equal to M_{cr}, into a final HyS or SS is denoted by the full circles connected by an arrow. In all the panels σ is taken equal to 30 MeV/fm^2 and $\gamma = 0$. The dashed lines show the gravitational red shift deduced for the X-ray compact sources EXO 0748-676 ($z = 0.35$) and 1E 1207.4-5209 ($z = 0.12 - 0.23$).

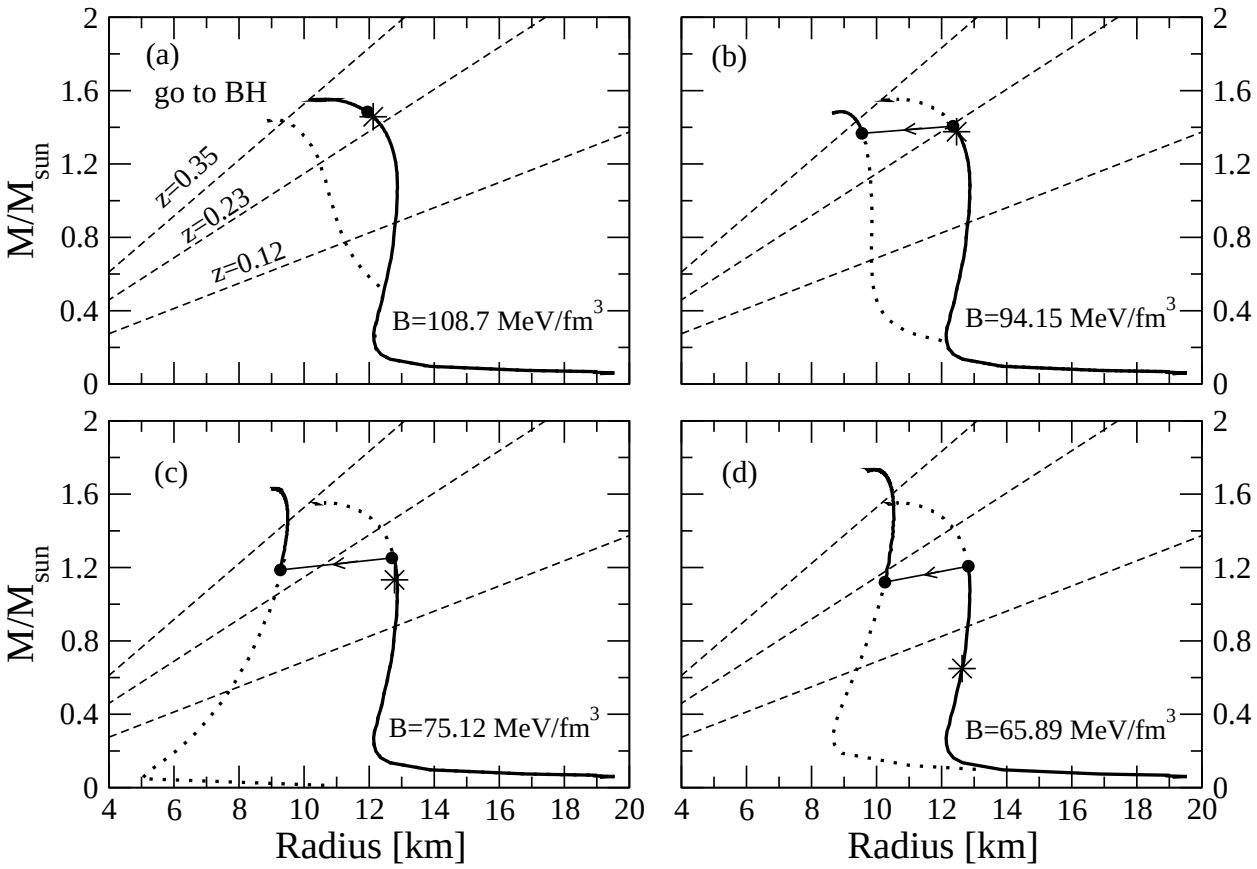

Fig. 7.— Same as Fig. 6 for the GM3+Bag model.

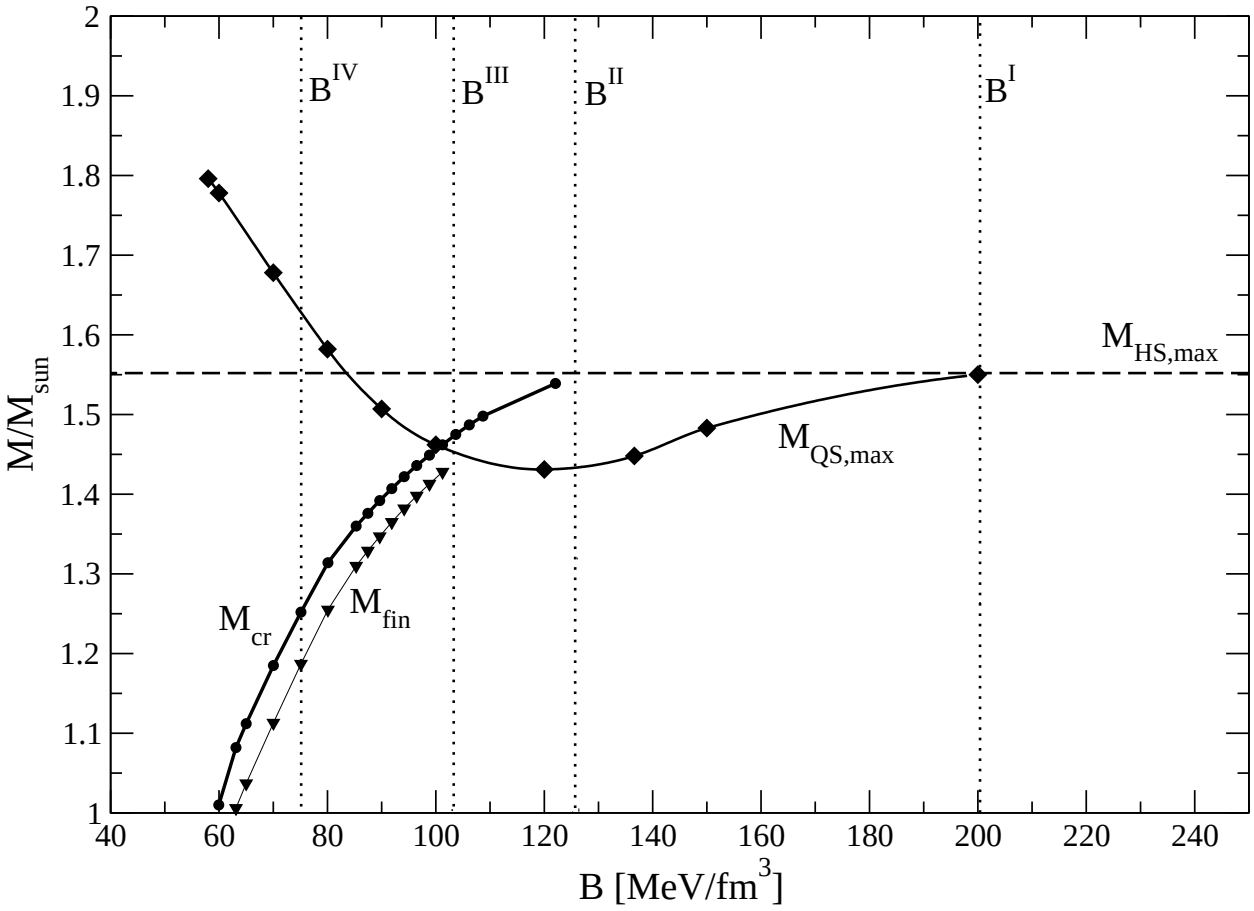

Fig. 8.— The maximum mass $M_{QS,max}$ for the quark star configuartions (HS or SS), the critical mass M_{cr} and the mass M_{fin} of the stable QS to which it evolves are plotted as a function of the bag constant B. The vertical doted lines labelled B^I – B^{IV} mark the boundary of different ranges of the bag constant which give a different astrophysical output for our scenario, as discussed in the text. The dashed horizontal line gives the value oh the maximum mass for the pure hadronic star sequence. All the results are relative to the GM3 model for the EOS for the hadronic phase, the surface tension σ is taken equal to 30 MeV/fm^2.

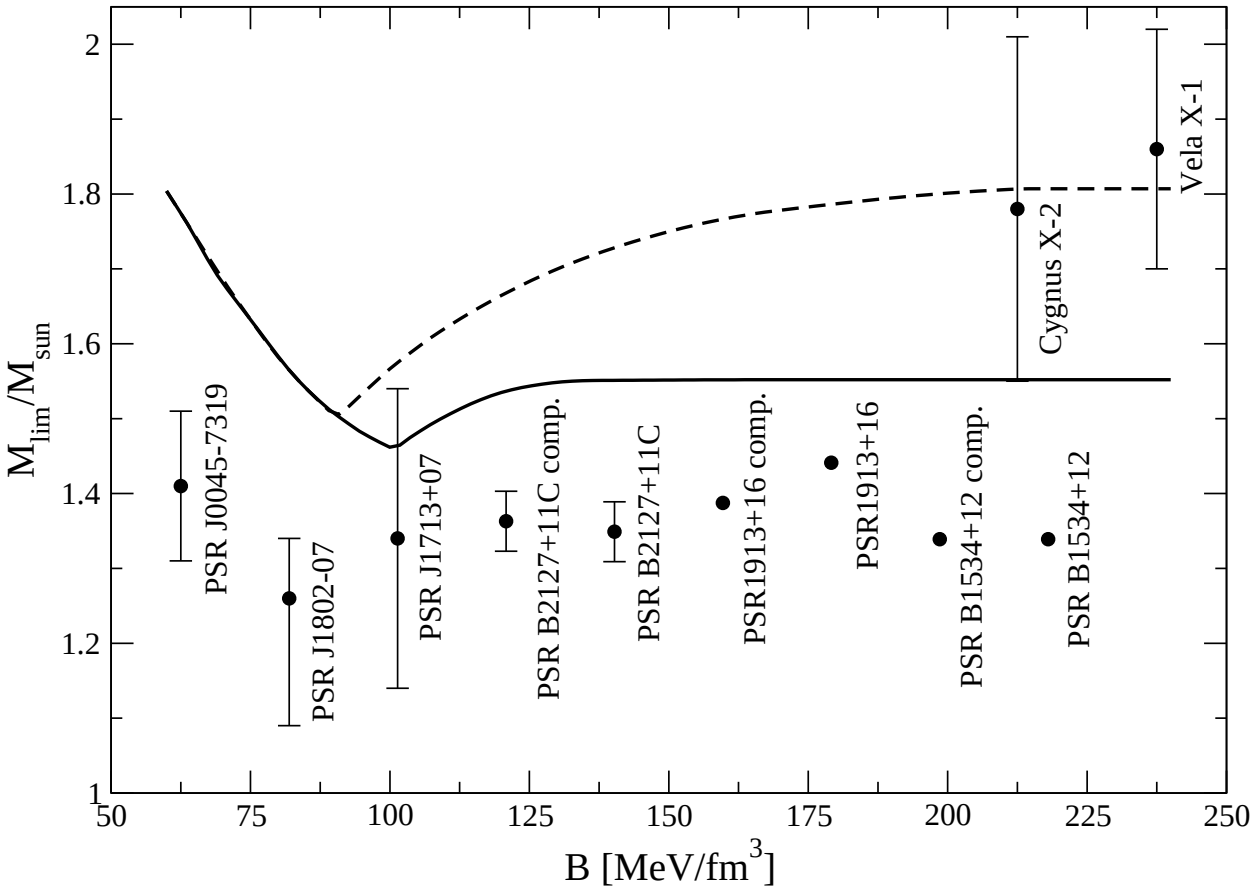

Fig. 9.— The limiting (gravitational) mass M_{lim}, according to generalized definition given in the present work, is plotted as a function of the Bag constant. Solid (dashed) lines show the results for the GM3+Bag (GM1+Bag) model. In both cases we take $\sigma = 30$ MeV/fm^2 and $\gamma = 0$. The values of some "measured" masses of compact stars in radio pulsars and in Vela X-1 and Cygnus X-2 are also reported for comparison.

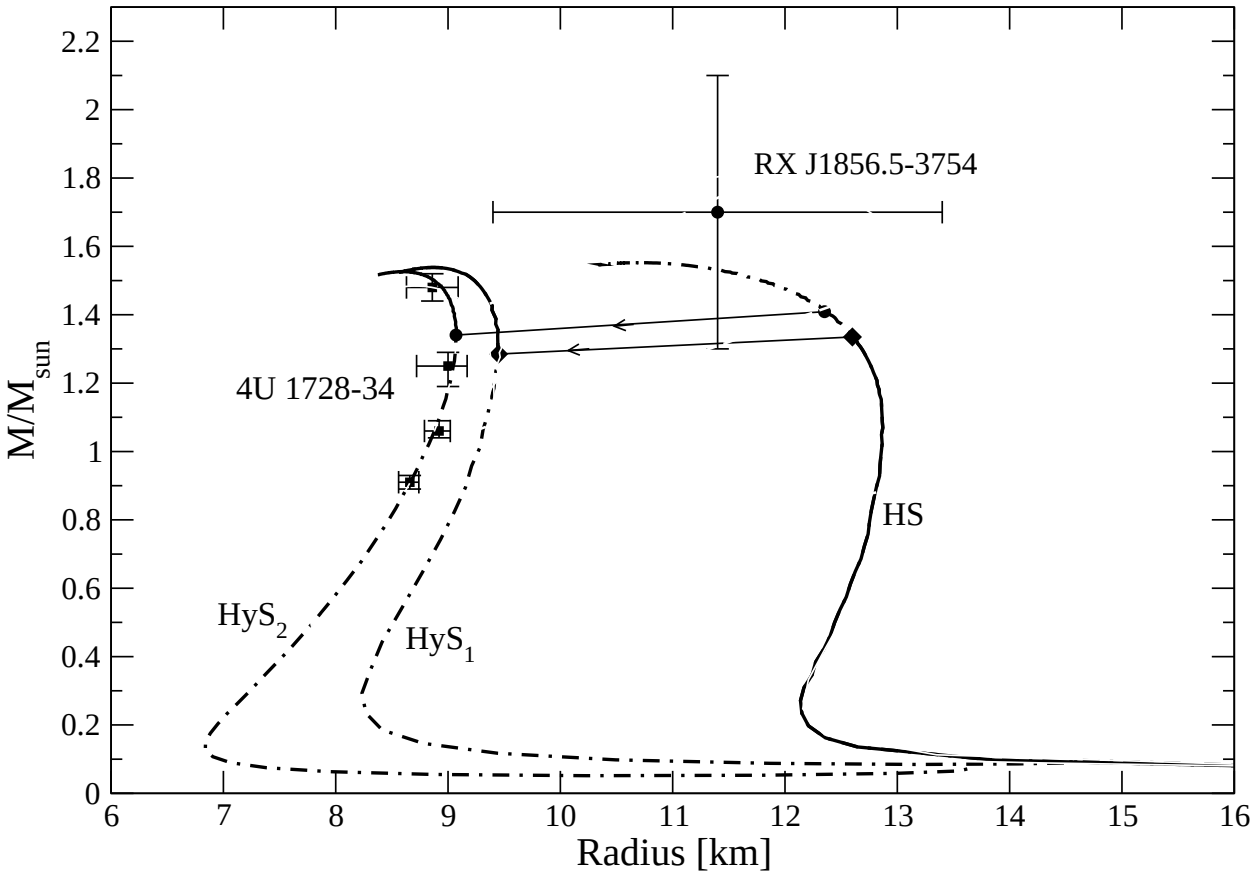

Fig. 10.— The radius and the mass for RX J1856.5-3754 (full circle with error bars labelled RX J1856.5-3754) obtained by Walter & Lattimer (2002) from fitting the multi-wave lenght spectral energy distribution. The radius and mass for 4U 1728-34, extracted by Shaposhnikov *et al.* ((66)) for different best-fits of the X-ray burst data, is shown by the filled circles with error bars (error contour for 90% confidence level). The curves labeled HS reprersents the MR relation for pure hadronic star with the GM3 equation of state. The curves labeled HyS_1 and HyS_2 are the MR curves for hybrid stars with the GM3+Bag model EOS, for $B = 85.29\mathrm{MeV/fm}^3$ and $m_s = 150$ MeV (HyS_1), and $B = 100\mathrm{MeV/fm}^3$ and $m_s = 0$ MeV (HyS_2). The full circles and diamonds on the MR curves represent the critical mass configuration (symbols on the HS curve) and the corresponding hybrid star configurations after the stellar conversion process (symbols on the HyS_1 and HyS_2 curves).